



Transcriptomic Response of *Nitrosomonas europaea* Transitioned from Ammonia- to Oxygen-Limited Steady-State Growth

Christopher J. Sedlacek,^{a,b} Andrew T. Giguere,^{a,c,g} Michael D. Dobie,^d Brett L. Mellbye,^d Rebecca V. Ferrell,^e Dagmar Woebken,^a Luis A. Sayavedra-Soto,^f Peter J. Bottomley,^{c,d} Holger Daims,^{a,b} Michael Wagner,^{a,b,g} Petra Pjevac^{a,h}

^aUniversity of Vienna, Centre for Microbiology and Environmental Systems Science, Division of Microbial Ecology, Vienna, Austria

^bUniversity of Vienna, The Comammox Research Platform, Vienna, Austria

^cDepartment of Crop and Soil Science, Oregon State University, Corvallis, Oregon, USA

^dDepartment of Microbiology, Oregon State University, Corvallis, Oregon, USA

^eDepartment of Biology, Metropolitan State University of Denver, Denver, Colorado, USA

^fDepartment of Botany and Plant Pathology, Oregon State University, Corvallis, Oregon, USA

^gCenter for Microbial Communities, Department of Chemistry and Bioscience, Aalborg University, Aalborg, Denmark

^hJoint Microbiome Facility of the Medical University of Vienna and the University of Vienna, Vienna, Austria

Christopher J. Sedlacek and Andrew T. Giguere contributed equally to this work. Author order was determined on the basis of seniority.

ABSTRACT Ammonia-oxidizing microorganisms perform the first step of nitrification, the oxidation of ammonia to nitrite. The bacterium *Nitrosomonas europaea* is the best-characterized ammonia oxidizer to date. Exposure to hypoxic conditions has a profound effect on the physiology of *N. europaea*, e.g., by inducing nitrifier denitrification, resulting in increased nitric and nitrous oxide production. This metabolic shift is of major significance in agricultural soils, as it contributes to fertilizer loss and global climate change. Previous studies investigating the effect of oxygen limitation on *N. europaea* have focused on the transcriptional regulation of genes involved in nitrification and nitrifier denitrification. Here, we combine steady-state cultivation with whole-genome transcriptomics to investigate the overall effect of oxygen limitation on *N. europaea*. Under oxygen-limited conditions, growth yield was reduced and ammonia-to-nitrite conversion was not stoichiometric, suggesting the production of nitrogenous gases. However, the transcription of the principal nitric oxide reductase (cNOR) did not change significantly during oxygen-limited growth, while the transcription of the nitrite reductase-encoding gene (*nirK*) was significantly lower. In contrast, both heme-copper-containing cytochrome *c* oxidases encoded by *N. europaea* were upregulated during oxygen-limited growth. Particularly striking was the significant increase in transcription of the B-type heme-copper oxidase, proposed to function as a nitric oxide reductase (sNOR) in ammonia-oxidizing bacteria. In the context of previous physiological studies, as well as the evolutionary placement of *N. europaea*'s sNOR with regard to other heme-copper oxidases, these results suggest sNOR may function as a high-affinity terminal oxidase in *N. europaea* and other ammonia-oxidizing bacteria.


IMPORTANCE Nitrification is a ubiquitous microbially mediated process in the environment and an essential process in engineered systems such as wastewater and drinking water treatment plants. However, nitrification also contributes to fertilizer loss from agricultural environments, increasing the eutrophication of downstream aquatic ecosystems, and produces the greenhouse gas nitrous oxide. As ammonia-oxidizing bacteria are the most dominant ammonia-oxidizing microbes in fertilized agricultural soils, understanding their responses to a variety of environmental conditions is essential for curbing the negative environmental effects of nitrification. Nota-

Citation Sedlacek CJ, Giguere AT, Dobie MD, Mellbye BL, Ferrell RV, Woebken D, Sayavedra-Soto LA, Bottomley PJ, Daims H, Wagner M, Pjevac P. 2020. Transcriptomic response of *Nitrosomonas europaea* transitioned from ammonia- to oxygen-limited steady-state growth. *mSystems* 5:e00562-19. <https://doi.org/10.1128/mSystems.00562-19>.

Editor Nick Bouskill, Lawrence Berkeley National Laboratory

Copyright © 2020 Sedlacek et al. This is an open-access article distributed under the terms of the [Creative Commons Attribution 4.0 International license](https://creativecommons.org/licenses/by/4.0/).

Address correspondence to Christopher J. Sedlacek, sedlacek@microbial-ecology.net.

 Adapting to oxygen-limited life! A transcriptomic look at AOB grown in substrate or oxygen limited chemostats. #Nitrocycle #Microbes #ASM

Received 9 September 2019

Accepted 4 December 2019

Published 14 January 2020

bly, oxygen limitation has been reported to significantly increase nitric oxide and nitrous oxide production during nitrification. Here, we investigate the physiology of the best-characterized ammonia-oxidizing bacterium, *Nitrosomonas europaea*, growing under oxygen-limited conditions.

KEYWORDS ammonia and oxygen limitation, ammonia-oxidizing bacteria, chemostat, nitrification, *Nitrosomonas europaea*, transcriptome

Nitrification is a microbially mediated aerobic process involving the successive oxidation of ammonia (NH_3) and nitrite (NO_2^-) to nitrate (NO_3^-) (1). In oxic environments, complete nitrification is accomplished through the complementary metabolisms of ammonia-oxidizing bacteria (AOB)/archaea (AOA) and nitrite-oxidizing bacteria (NOB) or by comammox bacteria (2, 3). The existence of nitrite-oxidizing archaea (NOA) has been proposed but not yet confirmed (4). Although an essential process during wastewater and drinking water treatment, nitrification is also a major cause of nitrogen (N) loss from N-amended soils. Nitrifiers increase N loss through the production of NO_3^- , which is more susceptible to leaching from soils than ammonium (NH_4^+), serves as terminal electron acceptor for denitrifiers, and contributes to the eutrophication of downstream aquatic environments (5).

In addition, ammonia oxidizers produce and release nitrogenous gases such as nitric (NO) and nitrous (N_2O) oxide during NH_3 oxidation at a wide range of substrate and oxygen (O_2) concentrations (6, 7). Nitrogenous gases are formed through enzymatic processes (8–13) but also by a multitude of chemical reactions that use the key metabolites of ammonia oxidizers, hydroxylamine (NH_2OH) and NO_2^- (or its acidic form HNO_2), as the main precursors (14, 15). AOB, in particular, release NO and N_2O either during NH_2OH oxidation (16–21) or via nitrifier denitrification—the reduction of NO_2^- to N_2O via NO (22–25). The first pathway is the dominant process at atmospheric O_2 levels, while the latter is more important under O_2 -limited (hypoxic) conditions (26, 27), where NO_2^- and NO serve as alternative sinks for electrons generated by NH_3 oxidation.

Nitrosomonas europaea strain ATCC 19718 was the first AOB to have its genome sequenced (28) and is widely used as a model organism in physiological studies of NH_3 oxidation and NO/ N_2O production in AOB (27, 29–36). The enzymatic background of NO and N_2O production in *N. europaea* is complex and involves multiple interconnected processes (Fig. 1). Most AOB harbor a copper-containing nitrite reductase, NirK, which is necessary for efficient NH_3 oxidation by *N. europaea* at atmospheric O_2 levels. NirK is also involved in but not essential for NO production during nitrifier denitrification in *N. europaea* (26, 27, 29, 35) and is upregulated in response to high NO_2^- concentrations (37). Moreover, two forms of membrane-bound cytochrome (cyt) *c* oxidases (cNOR and sNOR) and three cytochromes, referred to as cyt P460 (CytL), cyt *c'* beta (CytS), and cyt c_{554} (CycA), have been implicated in N_2O production in *N. europaea* and other AOB (12, 24, 32, 38–40). However, the involvement of cyt c_{554} in N_2O production has recently been disputed (41). Finally, recent research has confirmed that the oxidation of NH_3 to NO_2^- in AOB includes the formation of NO as an obligate intermediate, produced by NH_2OH oxidation via the hydroxylamine dehydrogenase (HAO) (20). The enzyme responsible for the oxidation of NO to NO_2^- (the proposed nitric oxide oxidase) has not yet been identified (40).

The production of NO and N_2O by *N. europaea*, grown under oxic as well as hypoxic (oxygen-limited) conditions, was previously demonstrated and quantified in multiple batch and chemostat culture studies (11, 12, 34, 35, 42, 43). Furthermore, recent studies have investigated the instantaneous rate of NO and N_2O production by *N. europaea* during the transition from oxic to oxygen-limited or anoxic conditions (12, 35, 36). Despite this large body of literature describing the effect of oxygen (O_2) limitation on NH_3 oxidation and NO/ N_2O production in *N. europaea*, little attention has been paid to the regulation of other processes under these conditions. Previous studies have utilized reverse transcription-quantitative PCR (RT-qPCR) assays to examine transcriptional

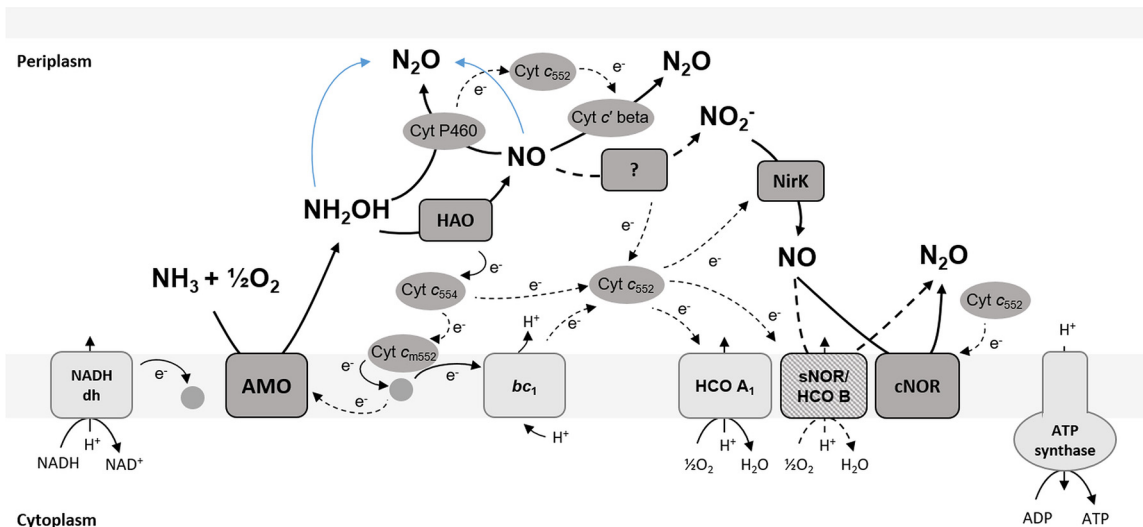


FIG 1 A simplified schematic of electron transport and NO/N₂O-producing pathways in *N. europaea*. Solid lines indicate confirmed and dashed lines indicate postulated reactions or electron transfer processes. Abiotic N₂O production is indicated in blue. NADH dh, NADH dehydrogenase (complex I); AMO, ammonia monoxygenase; HAO, hydroxylamine dehydrogenase; NirK, nitrite reductase; *bc*₁, cytochrome *bc*-I complex (complex III); HCO A₁, heme-copper-containing *cytochrome c* oxidase A1-type (complex IV); sNOR/HCO B, heme-copper-containing NO reductase/heme-copper-containing cytochrome *c* oxidase B-type (complex IV); cNOR, heme-iron-containing nitric oxide reductase.

patterns of specific mainly N cycle-related genes in AOB grown under O₂-limited conditions (34, 36, 44). To date, no study has evaluated the global transcriptomic response of *N. europaea* to O₂-limited growth. However, research on the effect of stressors other than reduced O₂ tension have demonstrated the suitability of transcriptomics for the analysis of physiological responses in AOB (43, 45–48).

N. europaea utilizes the Calvin-Benson-Bassham (CBB) cycle to fix inorganic carbon (28, 49). Whereas all genome-sequenced AOB appear to use the CBB cycle, differences exist in the number of copies of ribulose-1,5-bisphosphate carboxylase/oxygenase (RuBisCO) genes encoded as well as the presence or absence of carbon dioxide (CO₂)-concentrating mechanisms (50–52). *N. europaea* harbors a single form IA green-like (high-affinity) RuBisCO enzyme and two carbonic anhydrases but no carboxysome-related genes (28). RuBisCO is considered to function optimally in hypoxic environments, as it also uses O₂ as a substrate and produces the off-path intermediate 2-phosphoglycolate (53, 54). However, the effects of O₂ limitation on the transcription of RuBisCO-encoding genes and resulting growth yield in AOB are still poorly understood.

In this study, we expand upon previous work investigating the effects of O₂ limitation on *N. europaea* by profiling the transcriptomic response to substrate (NH₃) versus O₂ limitation. *N. europaea* was grown under steady-state NH₃- or O₂-limited conditions, which allowed for the investigation of differences in transcriptional patterns between growth conditions. We observed a downregulation of genes associated with CO₂ fixation as well as increased expression of two distinct heme-copper-containing cytochrome *c* oxidases (HCOs) during O₂-limited growth. Our results provide new insights into how *N. europaea* physiologically adapts to thrive in O₂-limited environments and identified putative key enzymes for future biochemical characterization.

RESULTS AND DISCUSSION

Growth characteristics. *N. europaea* was grown as a continuous steady-state culture under both NH₃- and O₂-limited growth conditions. During NH₃-limited steady-state growth, the culture was kept oxidic with a constant supply of filtered atmospheric air, was continuously stirred (400 rpm), and contained a standing NO₂⁻ concentration of ~60 mmol liter⁻¹. *N. europaea* grown under NH₃-limited conditions consumed

~98% of substrate provided; therefore, cultures were considered to have nonlimiting amounts of O₂ (Table 1). In contrast, during O₂-limited steady-state growth, no additional air inflow was provided, but the stirring was increased (800 rpm) to facilitate O₂ transfer between the headspace and growth medium. As a consequence of O₂ limitation, the medium contained standing concentrations (~30 mmol liter⁻¹) of both NH₄⁺ and NO₂⁻ (Fig. 2; Table 1).

During NH₃-limited steady-state growth (days 7 to 16) (Fig. 2), *N. europaea* stoichiometrically oxidized all supplied NH₄⁺ to NO₂⁻ (N balance = 61.0 ± 1.7 mmol liter⁻¹) and maintained an optical density at 600 nm (OD₆₀₀) of 0.15 ± 0.01 (Table 1). During O₂-limited steady-state growth (days 23 to 32) (Fig. 2), *N. europaea* was able to consume on average 31.1 ± 1.5 mmol liter⁻¹ (51.8%) of the supplied NH₄⁺ and maintained an OD₆₀₀ of 0.07 ± 0.01 (Table 1). A decrease in OD₆₀₀ was expected, as the O₂-limited culture oxidized less total substrate (NH₄⁺), resulting in less biomass produced. The conversion of NH₄⁺ to NO₂⁻ was not stoichiometric during O₂-limited growth, as only 77.5% (24.1 ± 0.8 mmol liter⁻¹) of the NH₄⁺ oxidized was measured as NO₂⁻ in the effluent, resulting in an N balance of 52.8 ± 1.8 mmol liter⁻¹ (Table 1). The significant difference ($P \leq 0.01$) in the N balance between NH₄⁺ consumed and NO₂⁻ formed during O₂-limited growth is in accordance with previous reports and likely due to increased N loss in the form of NH₂OH, NO, and N₂O under O₂-limited conditions (12, 35, 42, 55).

The dilution rate (0.01 h⁻¹) of the chemostat was kept constant during both NH₃- and O₂-limited growth, and resulted in 14.4 mmol day⁻¹ NH₄⁺ delivered into the chemostat. On days 9, 10, and 11, which were sampled for NH₃-limited growth transcriptomes, *N. europaea* consumed NH₃ at a rate (q_{NH_3}) of 24.73 ± 0.53 mmol g (dry cell weight)⁻¹ h⁻¹ with an apparent growth yield (Y) of 0.40 ± 0.01 g (dry cell weight) mol⁻¹ NH₃. During days sampled for O₂-limited growth transcriptomes (days 28, 29, and 30), the q_{NH_3} was significantly higher (28.51 ± 1.13 mmol g [dry cell weight]⁻¹ h⁻¹; $P \leq 0.05$), while Y was significantly lower (0.35 ± 0.01 g [dry cell weight] mol⁻¹ NH₃; $P \leq 0.05$). When the whole 10-day NH₃- and O₂-limited steady-state growth periods were considered, the q_{NH_3} and Y trends remained statistically significant ($P \leq 0.05$) (Table 1). Overall, NH₃ oxidation was less efficiently coupled to biomass production under O₂-limited growth conditions.

Global transcriptomic response of *N. europaea* to growth under NH₃- versus O₂-limited conditions. Under both NH₃- and O₂-limited growth conditions, transcripts mapping to 2,535 of 2,572 protein-coding genes (98.5%) and 3 RNA-coding genes (*ffs*, *rnpB*, and transfer-messenger RNA [tmRNA]) were detected. Many of the 37 genes not detected encode phage elements or transposases, some of which may have been excised from the genome in the >15 years of culturing since genome sequencing (see Data Set S1 in the supplemental material). In addition, no tRNA transcripts were detected. The high proportion of transcribed genes is in line with recent *N. europaea* transcriptomic studies, where similarly high fractions of transcribed genes were detected (43, 48). A significant difference in transcript levels between growth conditions was detected for 615 (~24%) of transcribed genes (see Fig. S1). Of these 615 genes, 435 (~71%) were present at higher levels, while 180 (~29%) were present at lower levels during O₂-limited growth. Genes encoding hypothetical proteins with no further functional annotation accounted for ~21% (130) of the differentially transcribed genes (Data Set S1). Steady-state growth under O₂-limited conditions mainly impacted the transcription of genes in clusters of orthologous groups (COGs) related to transcription and translation, ribosome structure and biogenesis, carbohydrate transport and metabolism, and energy production and conversion (Fig. 3).

Universal and reactive oxygen stress. The transcript levels of various chaperone proteins and sigma factors considered to be involved in the general stress response in *N. europaea* (45) differed between NH₃- and O₂-limited growth, with no discernible trend of regulation (see Table S2; Data Set S1). Overall, prolonged exposure to O₂ limitation did not seem to induce a significantly increased general stress response in

TABLE 1 Comparison of *N. europaea* growth characteristics and NH_4^+ to NO_2^- conversion stoichiometry during NH_3^- and O_2 -limited steady-state growth

Growth condition	Period (days)	OD_{600}^a	Input NH_3^b (mmol day $^{-1}$)	NH_3 consumed a (mmol day $^{-1}$)	Steady-state a NH_4^+ (mmol liter $^{-1}$)	Steady-state a NO_2^- (mmol liter $^{-1}$)	N balance c,d (mmol)	Ammonia oxidation rate a,d (q_{NH_3}) (mmol g [dry cell weight] $^{-1}$ h $^{-1}$)	Apparent growth yield a,d (Y) (g [dry cell weight] $^{-1}$ mol $^{-1}$ NH_3)
NH_3 limited	7–16	0.15 ± 0.01	14.4	14.2 ± 0.1	0.9 ± 0.5	60.1 ± 1.4	61.0 ± 1.7 A	24.04 ± 0.93 C	0.42 ± 0.02 C
	9–11	0.15 ± 0.004	14.4	14.2 ± 0.1	0.9 ± 0.4	59.1 ± 1.4	60.0 ± 1.8 c	24.73 ± 0.53 c	0.40 ± 0.01 c
O_2 limited growth	23–32	0.07 ± 0.01	14.4	7.5 ± 0.4	28.9 ± 1.5	24.1 ± 0.8	52.8 ± 1.8 B	26.44 ± 2.28 D	0.38 ± 0.03 D
	28–30	0.07 ± 0.0005	14.4	7.5 ± 0.3	28.6 ± 1.1	24.3 ± 1.4	52.9 ± 2.4 d	28.51 ± 1.13 d	0.35 ± 0.01 d

^a Average values from 3 sampling days or 10-day steady-state period, ± standard deviations (see Table S1 in the supplemental material).

^b The NH_4^+ concentration of the influent medium (60 mmol liter $^{-1}$) multiplied by the influx rate (0.24 liter day $^{-1}$).

^c Sum of effluent NH_4^+ and NO_2^- concentrations.

^d Letters A and B represent highly significant differences ($P \leq 0.01$), and letters C and D represent significant differences ($P \leq 0.05$) within parameters. Capital letters represent comparisons between 10-day periods, whereas lowercase letters represent comparisons between 3-day periods.

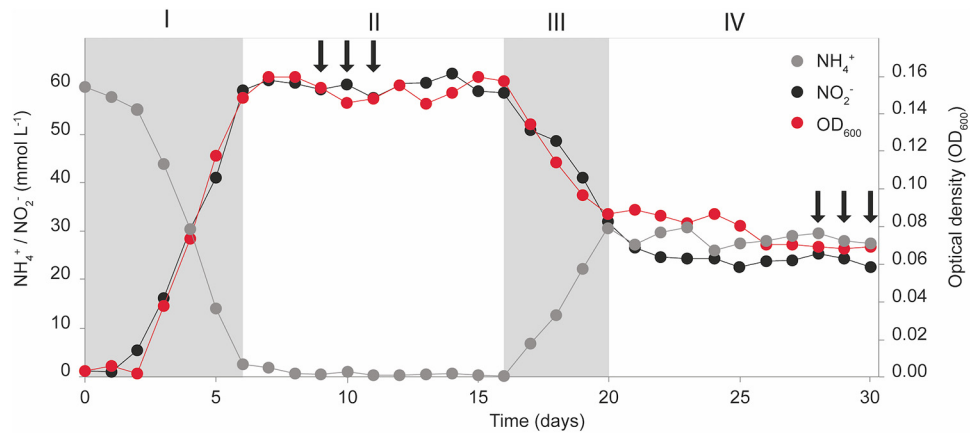


FIG 2 *N. europaea* culture dynamics and sampling scheme. *N. europaea* grown in a chemostat operated in batch mode (I), under steady-state NH_3 -limited conditions as a continuous culture (II), transitioning from NH_3 -limited to O_2 -limited steady-state growth as a continuous culture (III), and under steady-state O_2 -limited conditions as a continuous culture (IV). Arrows indicate transcriptome sampling points during NH_3 -limited (days 9, 10, and 11) and O_2 -limited (days 28, 29, and 30) steady-state growth.

N. europaea. Key genes involved in oxidative stress defense (superoxide dismutase, catalase, peroxidases, and thioredoxins) were transcribed at lower levels during O_2 -limited growth, as expected (Table S2; Data Set S1). Surprisingly, rubredoxin (NE1426) and a glutaredoxin family protein-encoding gene (NE2328) did not follow this trend and were transcribed at significantly higher levels (2.8- and 1.8-fold, respectively) during O_2 -limited growth (Table S2). Although their role in *N. europaea* is currently unresolved, both have been proposed to be involved in cellular oxidative stress response (56, 57), iron homeostasis (58, 59), or both.

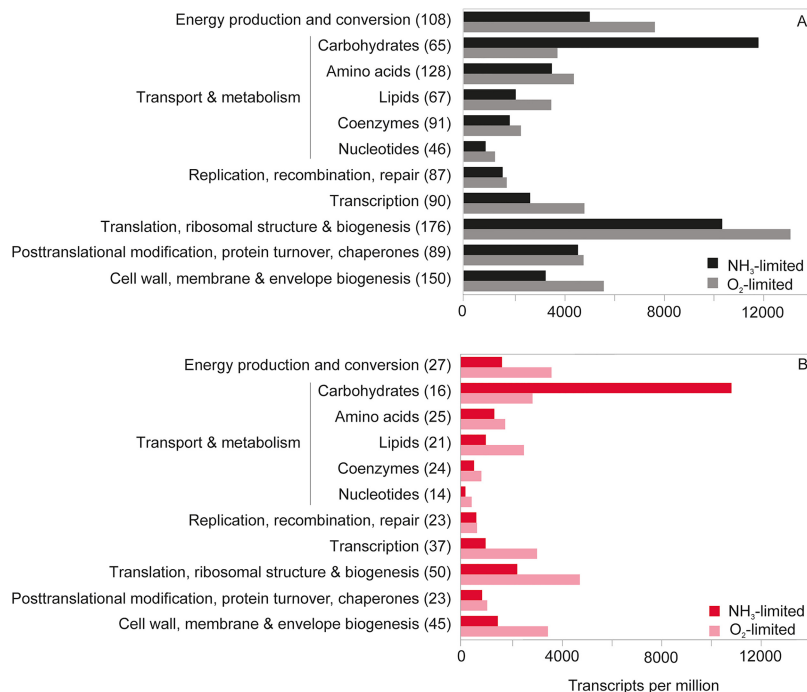


FIG 3 The sum of transcripts per million (TPM) for protein-coding genes transcribed in given COG categories (number of transcribed genes per category is given in parentheses) in the *N. europaea* transcriptomes. (A) Contributions and numbers of all transcribed genes in a given COG category. (B) Contributions and numbers of statistically significantly differentially transcribed genes in a given COG category.

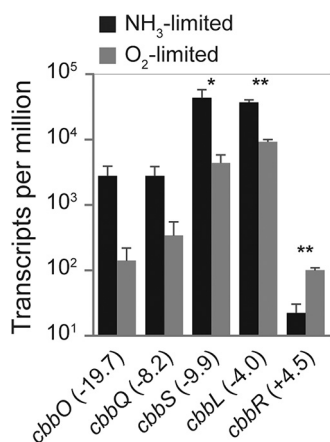


FIG 4 Mean TPMs of all RuBisCO-encoding genes (*cbbOQSL*) and the corresponding transcriptional regulator (*cbbR*) in *N. europaea*. The fold changes of gene transcription between NH₃- versus O₂-limited growth are given in parentheses. Error bars represent the standard deviations between replicate samples ($n = 3$) for each growth condition. A Welch's t test was used to determine significantly differentially transcribed genes. *, $P < 0.05$; **, $P < 0.01$. For gene annotations, refer to Table S2 in the supplemental material.

Carbon fixation and carbohydrate and storage compound metabolism. There was a particularly strong effect of O₂-limited growth on the transcription of several genes related to CO₂ fixation (Fig. 3B). The four genes of the RuBisCO-encoding *cbb* operon (*cbbOQSL*) were among the genes displaying the largest decrease in detected transcript numbers (Fig. 4; Table S2). Correspondingly, the transcriptional repressor of the *cbb* operon (*cbbR*) was transcribed at 4.5-fold higher levels (Fig. 4; Table S2). This agrees with the previously reported decrease in transcription of the *N. europaea* *cbbOQSL* operon in O₂-limited batch culture experiments (60). The reduced transcription of RuBisCO-encoding genes potentially reflects a decreased RuBisCO enzyme concentration needed to maintain an equivalent CO₂ fixation rate during O₂-limited growth. Since O₂ acts as a competing substrate for the RuBisCO active site, the CO₂-fixing carboxylase reaction proceeds more efficiently at lower O₂ concentrations (53, 61, 62). When *N. europaea* is grown under CO₂ limitation, the transcription of RuBisCO-encoding genes increases significantly (43, 60, 63). Due to the absence of carboxysomes, *N. europaea* appears to regulate CO₂ fixation at the level of RuBisCO enzyme concentration.

Genes encoding the remaining enzymes of the CBB pathway and carbonic anhydrases were not significantly differentially regulated, with the exception of the transketolase-encoding *cbbT* gene (Table S2). Likewise, almost no differences in transcription were observed for the majority of genes in other central metabolic pathways (glycolysis/gluconeogenesis, tricarboxylic acid [TCA] cycle) (Data Set S1). As the specific growth rate of *N. europaea* was kept constant during both NH₃- and O₂-limited growth, it is not surprising that genes associated with these core catabolic pathways were transcribed at comparable levels.

Differential transcription of polyphosphate (PP) metabolism-related genes suggests an increased accumulation of PP storage during O₂-limited growth. Transcripts of the polyphosphate kinase (*ppk*) involved in PP synthesis were detected in significantly higher numbers (2.1-fold), while transcription of the gene encoding the PP-degrading exopolyphosphatase (*ppx*) did not change (Table S2). Indeed, *N. europaea* was previously shown to accumulate PP when ATP generation (NH₃ oxidation) and ATP consumption become uncoupled and surplus ATP is available (64). As the specific growth rate was kept constant throughout the experiment, PP accumulation could be a result of increased efficiency in ATP-consuming pathways, such as CO₂ fixation or oxidative stress-induced repair. A decrease in the reaction flux through the energetically wasteful oxygenase reaction catalyzed by RuBisCO could result in surplus ATP being diverted to PP production.

Energy conservation. Genes encoding the known core enzymes of the NH_3 oxidation pathway in *N. europaea* were all highly transcribed during both NH_3 - and O_2 -limited growth (Table S2). These included ammonia monooxygenase (AMO; *amoCAB* operons and the singleton *amoC* gene) and the genes encoding HAO (*haoBA*) and the accessory *cyt*_{c554} (*cycA*) and *cyt*_{c552} (*cycX*). Due to a high level of sequence conservation among the multiple AMO and HAO operons (65), it is not possible to decipher the transcriptional responses of paralogous genes in these clusters. Therefore, we report the regulation of AMO and HAO operons as single units (Table S2). The transcript numbers of genes in the AMO operons decreased up to 3.3-fold during O_2 -limited growth, while transcripts of the singleton *amoC* were present at 1.9-fold higher levels. However, these transcriptional differences were not statistically significant. The HAO cluster genes were also not significantly differentially transcribed (Table S2).

Previous research has shown that transcription of AMO, and to a lesser extent of HAO, is induced by NH_3 in a concentration-dependent manner (66). In contrast, other studies have reported an increase in *amoA* transcription by *N. europaea* following substrate limitation (44, 67). Furthermore, *N. europaea* has been reported to increase *amoA* and *haoA* transcription during growth under low- O_2 conditions (34). However, exposure to repeated transient anoxia did not significantly change *amoA* or *haoA* mRNA levels (36). As both NH_3 and O_2 limitation were previously shown to induce transcription of AMO- and HAO-encoding genes, the high transcription levels observed here under both NH_3 - and O_2 -limited steady-state growth conditions are not surprising.

The periplasmic red copper protein nitrosocyanin (NcyA) was among the most highly transcribed genes under both NH_3 - and O_2 -limited growth conditions (Table S2). Nitrosocyanin has been shown to be expressed at levels similar to those of other nitrification and electron transport proteins (68) and is among the most abundant proteins commonly found in AOB proteomes (47, 69). To date, the nitrosocyanin-encoding gene *ncyA* has been identified only in AOB genomes (24) and has been proposed as a candidate for the nitric oxide oxidase (40). However, as comammox *Nitrospira* do not encode *ncyA* (2, 3, 13), nor do all genome-sequenced AOB (70), nitrosocyanin cannot be the NO oxidase in all ammonia oxidizers. In this study, a slight (1.7-fold) but not statistically significantly higher number of *ncyA* transcripts was detected during O_2 -limited growth (Table S2). This agrees with a previous study comparing *ncyA* mRNA levels in *N. europaea* continuous cultures grown under high- and low- O_2 conditions (44). However, *N. europaea* performing pyruvate-dependent NO_2^- reduction also significantly upregulated *ncyA*, while transcription of *amoA* and *haoA* decreased (44). Overall, there is evidence for an important role of nitrosocyanin in NH_3 oxidation or electron transport in AOB, but further experiments are needed to elucidate its exact function.

Three additional cytochromes are considered to be involved in the ammonia-oxidizing pathway of *N. europaea*: (i) *cyt*_{c552} (*cycB*), essential for electron transfer; (ii) *cyt* P460 (*cytL*), responsible for N_2O production from NO and hydroxylamine (39); and (iii) *cyt* c'-beta (*cytS*), hypothesized to be involved in N oxide detoxification and metabolism (24, 71). All three were among the most highly transcribed genes (top 20%) under both growth conditions (Table S2). In this study, *cytS* was transcribed at significantly lower levels (2.3-fold) during O_2 -limited growth. However, transcription levels of *cycB* and *cytL* were not significantly different (Table S2). While the *in vivo* function of *cytS* remains elusive, it is important to note that in contrast to *ncyA*, the *cytS* gene is present in all sequenced AOB and comammox *Nitrospira* genomes (12, 13, 52). The ubiquitous detection of *cytS* in genomes of all AOB, comammox *Nitrospira*, and in methane-oxidizing bacteria capable of NH_3 oxidation (72) indicates that *cyt* c'-beta might play an important yet unresolved role in bacterial aerobic NH_3 oxidation.

Nitrifier denitrification. During O_2 -limited growth, *N. europaea* either performs nitrifier denitrification or experiences a greater loss of N intermediates such as NH_2OH (73) or NO (20), which leads to the observed N imbalance between total NH_4^+

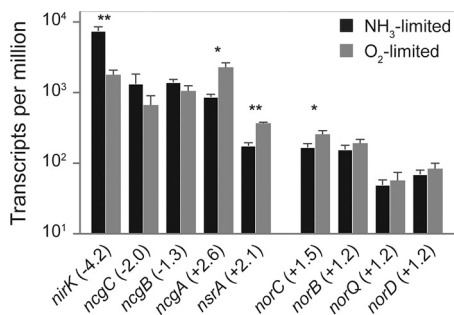


FIG 5 Mean TPMs of genes encoding the NirK and cNOR gene clusters in *N. europaea*. The fold changes of gene transcription between NH₃- versus O₂-limited growth are given in parentheses. Error bars represent the standard deviations between replicate samples ($n = 3$) for each growth condition. A Welch's *t* test was used to determine significantly differentially transcribed genes. *, $P < 0.05$; **, $P < 0.01$. For gene annotations refer to Table S2.

consumed and NO₂⁻ produced (Fig. 2; Table 1). The Cu-containing NO₂⁻ reductase NirK and the iron-containing membrane-bound cyt *c*-dependent NO reductase (cNOR; NorBC) are considered to be the main nitrifier denitrification enzymes (24, 35). *N. europaea* NirK plays an important role in both nitrifier denitrification and NH₃ oxidation (27) and is known to be expressed during both O₂-replete and -limited growth (29, 30, 35). However, under O₂-limited conditions, *nirK* was among the genes with the largest decrease in transcript numbers (4.2-fold) observed in this study (Fig. 5; Table S2). In *N. europaea*, *nirK* transcription is regulated via the nitrite-sensitive transcriptional repressor *nsrA* (30). Thus, in contrast to the *nirK* of many denitrifiers (74), *nirK* transcription in *N. europaea* is regulated in response to NO₂⁻ concentration and not NO or O₂ availability (31, 34, 48). The reduced O₂ supply during O₂-limited growth resulted in an ~50% decrease in total NH₃ oxidized and an ~60% reduction in steady-state NO₂⁻ concentration (Fig. 2; Table 1). The decrease in NO₂⁻ concentration during O₂-limited growth likely induced the transcription of *nsrA*, which was significantly (2.1-fold) upregulated (Fig. 5; Table S2). Therefore, the large decrease in *nirK* transcription observed here was likely due to the lower NO₂⁻ concentrations and not a direct reflection of overall nitrifier denitrification activity. In more natural nitrifying systems (e.g., agricultural soils or wastewater treatment plants [WWTPs]) changes in NO₂⁻ concentration could have a greater effect on AOB *nirK* expression than O₂ availability. However, it should be noted that environmental NO₂⁻ concentrations are unlikely to reach those observed in this study (30 to 60 mmol liter⁻¹ NO₂⁻).

Regulation of *nirK* transcription in response to primarily NO₂⁻ and not O₂ concentration is consistent with the observation that NirK is not essential for NO₂⁻ reduction to NO in *N. europaea*. This supports the hypothesis that a not-yet-identified nitrite reductase is present in this organism. Previously, it was shown that *N. europaea nirK* knockout mutants are still able to enzymatically produce NO and N₂O (29, 35), even if hydrazine is oxidized by HAO instead of hydroxylamine as an electron donor (35). In addition, NO and N₂O formation have also been observed in the AOB *Nitrosomonas communis* that does not encode *nirK* (12). The other three genes in the NirK cluster (*ncgCBA*) were differentially transcribed, with *ncgC* and *ncgB* being transcribed at lower levels (2- and 1.3-fold, respectively), while *ncgA* was transcribed at a significantly higher level (2.6-fold) during O₂-limited growth. The role of *ncgCBA* in *N. europaea* has not been fully elucidated, but all three genes were previously implicated in the metabolism or tolerance of N oxides and NO₂⁻ (31).

In contrast, transcripts of the *norCBQD* gene cluster, encoding the iron-containing cyt *c*-dependent cNOR-type NO reductase, were present at slightly higher (1.2- to 1.5-fold) but not significantly different levels during O₂-limited growth (Fig. 5; Table S2). Previous research has demonstrated that in *N. europaea*, cNOR functions as the main NO reductase under anoxic and hypoxic conditions (35). Interestingly, all components of the proposed alternative heme-copper-containing NO reductase (sNOR), including

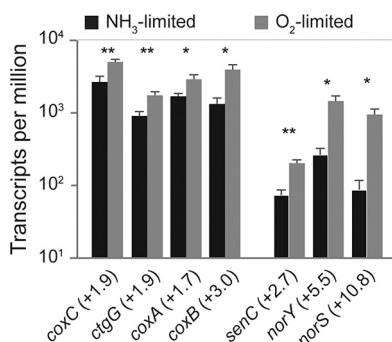


FIG 6 Mean TPMs of all genes encoding the A1-type and B-type HCO in *N. europaea*. The fold changes of gene transcription between NH₃- versus O₂-limited growth are given in parentheses. Error bars represent the standard deviations between replicate samples ($n = 3$) for each growth condition. A Welch's t test was used to determine significantly differentially transcribed genes. *, $P < 0.05$; **, $P < 0.01$. For gene annotations, refer to Table S2.

the NO/low-oxygen sensor *senC* (24), were transcribed at significantly higher levels (2.7- to 10.8-fold) during O₂-limited growth (Fig. 6; Table S2). Therefore, it is possible that the phenotype describing cNOR as the main NO reductase in *N. europaea* (35) was a product of short incubation times and that during longer term O₂-limited conditions, sNOR contributes to NO reduction during nitrifier denitrification. Another possibility is that the increased transcription of sNOR observed here during O₂-limited growth is primarily related to respiration and not NO reductase activity.

Respiratory chain and terminal oxidases. *N. europaea* harbors a low-affinity cytochrome *c* *aa*₃ (A1 type) HCO but not a high-affinity *cbb*₃-type (C type) cytochrome *c* HCO harbored by other AOB such as *N. europaea* or *Nitrosomonas* sp. GH22 (28, 50, 52). Significantly higher numbers of transcripts (1.7- to 3.0-fold) of all three subunits of the cytochrome *c* *aa*₃ HCO and the cytochrome *c* oxidase assembly gene *ctaG* were detected during O₂-limited growth (Fig. 6; Table S2). Increased transcription of the terminal oxidase was expected, as it is a common bacterial response to O₂ limitation (75). In addition, transcripts of all three subunits of the proton translocating cytochrome *bc*-1 complex (complex III) were present in higher numbers (Table S2). The genes encoding NADPH dehydrogenase (complex I) and ATP synthase (complex V) were transcribed at similar levels during both growth conditions (Table S2).

As mentioned above, transcripts of both subunits of sNOR (*norSY*, previously called *coxB*_{2A2}), and the NO/low-oxygen sensor *senC* were present at significantly higher numbers (2.7- to 10.8-fold) during O₂-limited growth (Fig. 6; Table S2). The NO reductase function of the sNOR enzyme complex was proposed based on domain similarities between NorY and NorB (24, 32). Yet, *norY* phylogenetically affiliates with and structurally resembles B-type HCOs (76). In addition, NorY does not contain the five well-conserved and functionally important NorB glutamate residues (77), which are present in the canonical NorB of *N. europaea*. All HCOs studied thus far can reduce O₂ to H₂O and couple this reaction to proton translocation, albeit B- and C-type HCOs translocate fewer protons per mole O₂ reduced than A-type HCOs (78). Notably, NO reduction to N₂O is a known side reaction of the A2-, B-, and C-type but not A1-type HCOs (79–81). The transcriptional induction of sNOR during O₂-limited growth reported here, as well as the high O₂ affinity of previously studied B-type HCOs (82), indicates that sNOR might function as a high-affinity terminal oxidase in *N. europaea* and possibly other sNOR-harboring AOB. Furthermore, functionally characterized B-type HCOs display a lower NO turnover rate than the more widespread high-affinity C-type HCOs (79, 80). Taken together, these observations indicate that B-type HCOs, such as sNOR, are ideal for scavenging O₂ during O₂-limited growth conditions that coincide with elevated NO concentrations, which would impart a fitness advantage for AOB growing under these conditions. Lastly, the NOR of *Roseobacter denitrificans* structurally resembles cNOR but contains an HCO-like heme-copper center in place of the heme-iron

center of canonical cNORs. Interestingly, this cNOR readily reduces O_2 to H_2O but displays very low NO reductase activity (83, 84). Therefore, in line with previous hypotheses (79, 83), the presence of a heme-copper center in NOR/HCO superfamily enzymes, such as the sNOR of *N. europaea*, may indicate O_2 reduction as the primary enzymatic function. Notably, a recent study provided the first indirect evidence of NO reductase activity of sNOR in the marine NOB, *Nitrococcus mobilis* (85). However, further research is needed to resolve the primary function of sNOR in nitrifying microorganisms.

Conclusions. In this study, we examined the transcriptional response of *N. europaea* to continuous growth under steady-state NH_3 - and O_2 -limited conditions. Overall, O_2 -limited growth resulted in a decreased growth yield but did not invoke a significant stress response in *N. europaea*. On the contrary, a reduced need for oxidative stress defense was evident. Interestingly, no clear differential regulation was observed for genes classically considered to be involved in aerobic NH_3 oxidation. In contrast, a strong decrease in transcription of RuBisCO-encoding genes during O_2 -limited growth was observed, suggesting that control of CO_2 fixation in *N. europaea* is exerted at the level of RuBisCO enzyme concentration. Furthermore, the remarkably strong increase in transcription of the genes encoding sNOR (B-type HCO) indicates this enzyme complex might function as a high-affinity terminal oxidase in *N. europaea* and other AOB. Overall, despite lower growth yield, *N. europaea* successfully adapts to growth under hypoxic conditions by regulating core components of its carbon fixation and respiration machinery.

MATERIALS AND METHODS

Cultivation. *N. europaea* ATCC 19718 was cultivated at 30°C as a batch and continuous chemostat culture as previously described (43, 48). Briefly, *N. europaea* was grown in mineral medium containing 30 mmol liter⁻¹ $(NH_4)_2SO_4$, 0.75 mmol liter⁻¹ $MgSO_4$, 0.1 mmol liter⁻¹ $CaCl_2$, and trace minerals (10 μ mol liter⁻¹ $FeCl_3$, 1.0 μ mol liter⁻¹ $CuSO_4$, 0.6 μ mol liter⁻¹ $Na_2Mo_4O_4$, 1.59 μ mol liter⁻¹ $MnCl_2$, 0.6 μ mol liter⁻¹ $CoCl_2$, 0.096 μ mol liter⁻¹ $ZnCl_2$). After sterilization by autoclaving, the medium was buffered by the addition of 6 ml liter⁻¹ autoclaved phosphate-carbonate buffer solution (0.52 mmol liter⁻¹ $NaH_2PO_4 \cdot H_2O$, 3.5 mmol liter⁻¹ KH_2PO_4 , 0.28 mmol liter⁻¹ Na_2CO_3 , pH adjusted to 7.0 with HCl).

For steady-state growth, a flowthrough bioreactor (Applikon Biotechnology) with a 1-liter working volume was inoculated with 2% (vol/vol) of an exponential-phase *N. europaea* batch culture. The bioreactor was set to “batch” mode until the NH_4^+ concentration reached <5 mmol liter⁻¹ (6 days) (see Table S1 in the supplemental material). Subsequently, the bioreactor was switched to continuous flow “chemostat” mode, at a dilution rate/specific growth rate (μ) of 0.01 h⁻¹ (doubling time = ~70 h), which was controlled by a peristaltic pump (Thermo Scientific). The culture was continuously stirred at 400 rpm, and the pH was automatically maintained at 7.0 ± 0.1 by addition of sterile 0.94 mol liter⁻¹ (10% [wt/vol]) Na_2CO_3 solution. Sterile-filtered (0.2 μ m) air, at a rate of 40 ml min⁻¹, was supplied during batch and NH_3 -limited steady-state growth. Once NH_3 -limited steady-state was reached (day 7), the chemostat was continuously operated under NH_3 -limited conditions for 10 days. To transition to O_2 -limited steady-state growth, after day 16, the air input was stopped, and the stirring speed was increased to 800 rpm to facilitate gas exchange between the medium and the headspace. The headspace was continuously replenished with O_2 by the passive diffusion of atmospheric air into the chemostat through open air inlets containing a sterile filter (0.2 μ m). O_2 -limited steady-state growth was achieved on day 23 as defined by the persistence of 26.4 to 31 mmol liter⁻¹ NH_4^+ and the accumulation of 22.8 to 25.5 mmol liter⁻¹ NO_2^- in the growth medium. The culture was continuously grown under these conditions for 10 days.

Sterile samples (~5 ml) were taken on a daily basis. Culture purity was assessed by periodically inoculating ~100 μ l of culture onto lysogeny broth (Sigma-Aldrich) agar plates, which were incubated at 30°C for at least 4 days. Any observed growth on agar plates was considered contamination, and those cultures were discarded. NH_4^+ and NO_2^- concentrations were determined colorimetrically (86), and cell density was determined spectrophotometrically (Beckman) by making optical density measurements at 600 nm (OD_{600}) (Table S1). Total biomass in grams (dry cell weight) per liter, substrate consumption rate (q_{NH_3}), and apparent growth yield (Y) were calculated as described in Mellbye et al. (43). To test for statistically significant differences in NH_4^+ to NO_2^- conversion stoichiometry, q_{NH_3} , and Y between NH_3 - and O_2 -limited steady-state growth, a Welch's *t* test was performed.

RNA extraction and transcriptome sequencing. For RNA extraction and transcriptome sequencing, three replicate samples (40 ml) were collected on three separate days during NH_3 -limited (days 9, 10, 11) and O_2 -limited (days 28, 29, 30) steady-state growth (Fig. 2). The samples were harvested by centrifugation (12,400 $\times g$, 30 min, 4°C), resuspended in RNeasy RLT buffer with 2-mercaptoethanol, and lysed with an ultrasonication probe (3.5 output, pulse of 30 s on/30 s off for 1 min; Heatsystems Ultrasonic Processor XL). RNA was extracted using the RNeasy minikit (Qiagen) followed by the MICROExpress-bacteria RNA Enrichment kit (Ambion/Life Technologies) according to the manufacturer's instructions.

Depleted RNA quality was assessed using the Bioanalyzer 6000 Nano Lab-Chip kit (Agilent Technologies). Sequencing libraries were constructed from at least 200 ng rRNA-depleted RNA with the TruSeq targeted RNA expression kit (Illumina), and 100-bp paired-end libraries were sequenced on a HiSeq 2000 (Illumina) at the Center for Genome Research and Biocomputing Core Laboratories (CGRB) at Oregon State University.

Transcriptome analysis. Paired-end transcriptome sequence reads were processed and mapped to open reading frames (ORFs) deposited at NCBI for the *N. europaea* ATCC 19718 (NC_004757.1) reference genome using the CLC Genomics Workbench (CLC bio) under default parameters as previously described (43). Residual reads mapping to the rRNA operon were excluded prior to further analysis. An additive consensus read count was manually generated for all paralogous genes. Thereafter, mapped read counts for each gene were normalized to the gene length in kilobases, and the resulting read per kilobase (RPK) values were converted to transcripts per million (TPM) (87). To test for statistically significant differences between transcriptomes obtained from NH₃- and O₂-limited steady-state growth, TPMs of biological triplicate samples were used to calculate *P* values based on a Welch's *t* test. The more stringent Welch's rather than the Student's *t* test was selected due to the limited number of biological replicates (88). Additionally, linear fold changes between average TPMs under both growth conditions for each expressed ORF were calculated. Transcripts with a *P* value of ≤ 0.05 and a transcription fold change of $\geq 1.5\times$ between conditions were considered present at significantly different levels.

Data availability. All retrieved transcriptome sequence data have been deposited in the European Nucleotide Archive (ENA) under the project accession number PRJEB31097.

SUPPLEMENTAL MATERIAL

Supplemental material is available online only.

FIG S1, PDF file, 1.7 MB.

TABLE S1, PDF file, 0.1 MB.

TABLE S2, PDF file, 0.1 MB.

DATA SET S1, XLSX file, 0.3 MB.

ACKNOWLEDGMENTS

We thank the Center for Genome Research and Biocomputing at Oregon State University for the sequencing services. We also thank Fillipa Sousa for helpful discussions.

This work was funded by Department of Energy (DOE) award ER65192 (co-principal investigators, L.A.S.-S. and P.J.B.). C.J.S., H.D., and M.W. were supported by the Comamox Research Platform of the University of Vienna. In addition, M.W. and C.J.S. were supported by the European Research Council (ERC) via the Advanced Grant project NITRICARE 294343, and C.J.S. and H.D. were supported by Austrian Science Fund (FWF) grant 30570-B29. A.T.G. and D.W. were supported by the ERC Starting Grant 636928, under the European Union's Horizon 2020 research and innovation program.

REFERENCES

- Kuypers MMM, Marchant HK, Kartal B. 2018. The microbial nitrogen-cycling network. *Nat Rev Microbiol* 16:263–276. <https://doi.org/10.1038/nrmicro.2018.9>.
- Daims H, Lebedeva EV, Pjevac P, Han P, Herbold C, Albertsen M, Jehmlich N, Palatinszky M, Vierheilig J, Bulaev A, Kirkegaard RH, von Bergen M, Rattei T, Bendinger B, Nielsen PH, Wagner M. 2015. Complete nitrification by *Nitrospira* bacteria. *Nature* 528:504–506. <https://doi.org/10.1038/nature16461>.
- van Kessel M, Speth DR, Albertsen M, Nielsen PH, den Camp HJO, Kartal B, Jetten MSM, Lucker S. 2015. Complete nitrification by a single microorganism. *Nature* 528:555–559. <https://doi.org/10.1038/nature16459>.
- Kitzinger K, Koch H, Lucker S, Sedlacek CJ, Herbold C, Schwarz J, Daebeler A, Mueller AJ, Lukumbuzya M, Romano S, Leisch N, Karst SM, Kirkegaard R, Albertsen M, Nielsen PH, Wagner M, Daims H. 2018. Characterization of the first “*Candidatus Nitrotoga*” isolate reveals metabolic versatility and separate evolution of widespread nitrite-oxidizing bacteria. *mBio* 9:e01186-18. <https://doi.org/10.1128/mBio.01186-18>.
- Galloway JN, Townsend AR, Erisman JW, Bekunda M, Cai Z, Freney JR, Martinelli LA, Seitzinger SP, Sutton MA. 2008. Transformation of the nitrogen cycle: recent trends, questions, and potential solutions. *Science* 320:889–892. <https://doi.org/10.1126/science.1136674>.
- Dundee L, Hopkins DW. 2001. Different sensitivities to oxygen of nitrous oxide production by *Nitrosomonas europaea* and *Nitrosolobus multiformis*. *Soil Biol Biochem* 33:1563–1565. [https://doi.org/10.1016/S0038-0717\(01\)00059-1](https://doi.org/10.1016/S0038-0717(01)00059-1).
- Shaw LJ, Nicol GW, Smith Z, Fear J, Prosser JI, Baggs EM. 2006. *Nitrosospira* spp. can produce nitrous oxide via a nitrifier denitrification pathway. *Environ Microbiol* 8:214–222. <https://doi.org/10.1111/j.1462-2920.2005.00882.x>.
- Ahn JH, Kwan T, Chandran K. 2011. Comparison of partial and full nitrification processes applied for treating high-strength nitrogen wastewaters: microbial ecology through nitrous oxide production. *Environ Sci Technol* 45:2734–2740. <https://doi.org/10.1021/es103534g>.
- Kool DM, Dolfig J, Wrage N, Van Groenigen JW. 2011. Nitrifier denitrification as a distinct and significant source of nitrous oxide from soil. *Soil Biol Biochem* 43:174–178. <https://doi.org/10.1016/j.soilbio.2010.09.030>.
- Santoro AE, Buchwald C, McIlvin MR, Casciotti KL. 2011. Isotopic signature of N₂O produced by marine ammonia-oxidizing archaea. *Science* 333:1282–1285. <https://doi.org/10.1126/science.1208239>.
- Stein LY. 2011. Surveying N₂O-producing pathways in bacteria, p 131–152. *In* Klotz MG (ed), *Methods in enzymology*. Academic Press, Waltham, MA.
- Kozłowski JA, Kits KD, Stein LY. 2016. Comparison of nitrogen oxide metabolism among diverse ammonia-oxidizing bacteria. *Front Microbiol* 7:1090. <https://doi.org/10.3389/fmicb.2016.01090>.
- Kits KD, Jung MY, Vierheilig J, Pjevac P, Sedlacek CJ, Liu S, Herbold C, Stein LY, Richter A, Wissel H, Brüggemann N, Wagner M, Daims H. 2019.

- Low yield and abiotic origin of N_2O formed by the complete nitrifier *Nitrospira inopinata*. *Nat Commun* 10:1836. <https://doi.org/10.1038/s41467-019-09790-x>.
14. Schreiber F, Wunderlin P, Udert KM, Wells GF. 2012. Nitric oxide and nitrous oxide turnover in natural and engineered microbial communities: biological pathways, chemical reactions, and novel technologies. *Front Microbiol* 3:372. <https://doi.org/10.3389/fmicb.2012.00372>.
 15. Heil J, Vereecken H, Brüggemann N. 2016. A review of chemical reactions of nitrification intermediates and their role in nitrogen cycling and nitrogen trace gas formation in soil. *Eur J Soil Sci* 67:23–39. <https://doi.org/10.1111/ejss.12306>.
 16. Hooper AB. 1968. A nitrite-reducing enzyme from *Nitrosomonas europaea*. Preliminary characterization with hydroxylamine as electron donor. *Biochim Biophys Acta* 162:49–65. [https://doi.org/10.1016/0005-2728\(68\)90213-2](https://doi.org/10.1016/0005-2728(68)90213-2).
 17. Hooper AB, Terry KR. 1977. Hydroxylamine oxidoreductase from *Nitrosomonas*: inactivation by hydrogen peroxide. *Biochemistry* 16: 455–459. <https://doi.org/10.1021/bi00622a018>.
 18. Hooper AB, Terry KR, Maxwell PC. 1977. Hydroxylamine oxidoreductase of *Nitrosomonas*. Oxidation of diethyldithiocarbamate concomitant with stimulation of nitrite synthesis. *Biochim Biophys Acta* 462:141–152. [https://doi.org/10.1016/0005-2728\(77\)90196-7](https://doi.org/10.1016/0005-2728(77)90196-7).
 19. Anderson IC, Poth M, Homstead J, Burdige D. 1993. A comparison of NO and N_2O production by the autotrophic nitrifier *Nitrosomonas europaea* and the heterotrophic nitrifier *Alcaligenes faecalis*. *Appl Environ Microbiol* 59:3525–3533.
 20. Caranto JD, Lancaster KM. 2017. Nitric oxide is an obligate bacterial nitrification intermediate produced by hydroxylamine oxidoreductase. *Proc Natl Acad Sci U S A* 114:8217–8222. <https://doi.org/10.1073/pnas.1704504114>.
 21. Mellbye BL, Giguere AT, Murthy GS, Bottomley PJ, Sayavedra-Soto LA, Chaplen FWR. 2018. Genome-scale, constraint-based modeling of nitrogen oxide fluxes during coculture of *Nitrosomonas europaea* and *Nitrobacter winogradskyi*. *mSystems* 3:e00170-17. <https://doi.org/10.1128/mSystems.00170-17>.
 22. Poth M, Focht DD. 1985. ^{15}N kinetic analysis of N_2O production by *Nitrosomonas europaea*: an examination of nitrifier denitrification. *Appl Environ Microbiol* 49:1134–1141.
 23. Wrage N, Velthof GL, van Beusichem ML, Oenema O. 2001. Role of nitrifier denitrification in the production of nitrous oxide. *Soil Biol Biochem* 33:1723–1732. [https://doi.org/10.1016/S0038-0717\(01\)00096-7](https://doi.org/10.1016/S0038-0717(01)00096-7).
 24. Klotz MG, Stein LY. 2008. Nitrifier genomics and evolution of the nitrogen cycle. *FEMS Microbiol Lett* 278:146–156. <https://doi.org/10.1111/j.1574-6968.2007.00970.x>.
 25. Giguere AT, Taylor AE, Suwa Y, Myrold DD, Bottomley PJ. 2017. Uncoupling of ammonia oxidation from nitrite oxidation: impact upon nitrous oxide production in non-cropped Oregon soils. *Soil Biol Biochem* 104: 30–38. <https://doi.org/10.1016/j.soilbio.2016.10.011>.
 26. Schmidt I, van Spanning RJM, Jetten M. 2004. Denitrification and ammonia oxidation by *Nitrosomonas europaea* wild-type, and NirK- and NorB-deficient mutants. *Microbiology* 150:4107–4114. <https://doi.org/10.1099/mic.0.27382-0>.
 27. Cantera JLL, Stein LY. 2007. Role of nitrite reductase in the ammonia-oxidizing pathway of *Nitrosomonas europaea*. *Arch Microbiol* 188: 349–354. <https://doi.org/10.1007/s00203-007-0255-4>.
 28. Chain P, Lamerdin J, Larimer F, Regala W, Lao V, Land M, Hauser L, Hooper A, Klotz M, Norton J, Sayavedra-Soto L, Arciero D, Hommes N, Whittaker M, Arp D. 2003. Complete genome sequence of the ammonia-oxidizing bacterium and obligate chemolithoautotroph *Nitrosomonas europaea*. *J Bacteriol* 185:2759–2773. <https://doi.org/10.1128/jb.185.9.2759-2773.2003>.
 29. Beaumont HJ, Hommes NG, Sayavedra-Soto LA, Arp DJ, Arciero DM, Hooper AB, Westerhoff HV, van Spanning R. 2002. Nitrite reductase of *Nitrosomonas europaea* is not essential for production of gaseous nitrogen oxides and confers tolerance to nitrite. *J Bacteriol* 184:2557–2560. <https://doi.org/10.1128/jb.184.9.2557-2560.2002>.
 30. Beaumont HJ, Lens SI, Reijnders WN, Westerhoff HV, van Spanning RJ. 2004. Expression of nitrite reductase in *Nitrosomonas europaea* involves NsrR, a novel nitrite-sensitive transcription repressor. *Mol Microbiol* 54:148–158. <https://doi.org/10.1111/j.1365-2958.2004.04248.x>.
 31. Beaumont HJ, Lens SI, Westerhoff HV, van Spanning RJ. 2005. Novel nirK cluster genes in *Nitrosomonas europaea* are required for NirK-dependent tolerance to nitrite. *J Bacteriol* 187:6849–6851. <https://doi.org/10.1128/JB.187.19.6849-6851.2005>.
 32. Cho CMH, Yan T, Liu X, Wu L, Zhou J, Stein LY. 2006. Transcriptome of a *Nitrosomonas europaea* mutant with a disrupted nitrite reductase gene (*nirK*). *Appl Environ Microbiol* 72:4450–4454. <https://doi.org/10.1128/AEM.02958-05>.
 33. Pellitteri-Hahn MC, Halligan BD, Scalf M, Smith L, Hickey WJ. 2011. Quantitative proteomic analysis of the chemolithoautotrophic bacterium *Nitrosomonas europaea*: comparison of growing-and energy-starved cells. *J Proteomics* 74:411–419. <https://doi.org/10.1016/j.jprotp.2010.12.003>.
 34. Yu R, Chandran K. 2010. Strategies of *Nitrosomonas europaea* 19718 to counter low dissolved oxygen and high nitrite concentrations. *BMC Microbiol* 10:70. <https://doi.org/10.1186/1471-2180-10-70>.
 35. Kozłowski JA, Price J, Stein LY. 2014. Revision of N_2O -producing pathways in the ammonia-oxidizing bacterium, *Nitrosomonas europaea* ATCC 19718. *Appl Environ Microbiol* 80:4930–4935. <https://doi.org/10.1128/AEM.01061-14>.
 36. Yu R, Perez-Garcia O, Lu H, Chandran K. 2018. *Nitrosomonas europaea* adaptation to anoxic-oxic cycling: insights from transcription analysis, proteomics and metabolic network modeling. *Sci Total Environ* 615: 1566–1573. <https://doi.org/10.1016/j.scitotenv.2017.09.142>.
 37. Cua LS, Stein LY. 2011. Effects of nitrite on ammonia-oxidizing activity and gene regulation in three ammonia-oxidizing bacteria. *FEMS Microbiol Lett* 319:169–175. <https://doi.org/10.1111/j.1574-6968.2011.02277.x>.
 38. Upadhyay AK, Hooper AB, Hendrich MP. 2006. NO reductase activity of the tetraheme cytochrome c_{554} of *Nitrosomonas europaea*. *J Am Chem Soc* 128:4330–4337. <https://doi.org/10.1021/ja055183+>.
 39. Caranto JD, Vilbert AC, Lancaster KM. 2016. *Nitrosomonas europaea* cytochrome P460 is a direct link between nitrification and nitrous oxide emission. *Proc Natl Acad Sci U S A* 113:14704–14709. <https://doi.org/10.1073/pnas.1611051113>.
 40. Lancaster KM, Caranto JD, Majer SH, Smith MA. 2018. Alternative bioenergy: updates to and challenges in nitrification metalloenzymology. *Joule* 2:421–441. <https://doi.org/10.1016/j.joule.2018.01.018>.
 41. McGarry JM, Pacheco A. 2018. Upon further analysis, neither cytochrome c_{554} from *Nitrosomonas europaea* nor its F156A variant display NO reductase activity, though both proteins bind nitric oxide reversibly. *J Biol Inorg Chem* 23:861–878. <https://doi.org/10.1007/s00775-018-1582-4>.
 42. Kester RA, De Boer W, Laanbroek HJ. 1997. Production of NO and N_2O by pure cultures of nitrifying and denitrifying bacteria during changes in aeration. *Appl Environ Microbiol* 63:3872–3877.
 43. Mellbye BL, Giguere A, Chaplen F, Bottomley PJ, Sayavedra-Soto LA. 2016. Steady-state growth under inorganic carbon limitation increases energy consumption for maintenance and enhances nitrous oxide production in *Nitrosomonas europaea*. *Appl Environ Microbiol* 82: 3310–3318. <https://doi.org/10.1128/AEM.00294-16>.
 44. Beyer S, Gilch S, Meyer O, Schmidt I. 2009. Transcription of genes coding for metabolic key functions in *Nitrosomonas europaea* during aerobic and anaerobic growth. *J Mol Microbiol Biotechnol* 16:187–197. <https://doi.org/10.1159/000142531>.
 45. Gvakharia BO, Permina EA, Gelfand MS, Bottomley PJ, Sayavedra-Soto LA, Arp DJ. 2007. Global transcriptional response of *Nitrosomonas europaea* to chloroform and chloromethane. *Appl Environ Microbiol* 73: 3440–3445. <https://doi.org/10.1128/AEM.02831-06>.
 46. Park S, Ely RL. 2008. Genome-wide transcriptional responses of *Nitrosomonas europaea* to zinc. *Arch Microbiol* 189:541–548. <https://doi.org/10.1007/s00203-007-0341-7>.
 47. Kartal B, Wessels HJ, van der Biezen E, Francoijs KJ, Jetten MS, Klotz MG, Stein LY. 2012. Effects of nitrogen dioxide and anoxia on global gene and protein expression in long-term continuous cultures of *Nitrosomonas europaea* C91. *Appl Environ Microbiol* 78:4788–4794. <https://doi.org/10.1128/AEM.00668-12>.
 48. Pérez J, Buchanan A, Mellbye B, Ferrell R, Chang JH, Chaplen F, Bottomley PJ, Arp DJ, Sayavedra-Soto LA. 2015. Interactions of *Nitrosomonas europaea* and *Nitrobacter winogradskyi* grown in co-culture. *Arch Microbiol* 197:79–89. <https://doi.org/10.1007/s00203-014-1056-1>.
 49. Sayavedra-Soto LA, Arp DJ. 2011. Ammonia-oxidizing Bacteria: their biochemistry and molecular biology, p 11–38. *In* Ward BB, Arp DJ, Klotz MG (ed). Nitrification. ASM Press, Washington, DC.
 50. Stein LY, Arp DJ, Berube PM, Chain PS, Hauser L, Jetten MS, Klotz MG, Larimer FW, Norton JM, Op den Camp HJ, Shin M, Wei X. 2007. Whole-genome analysis of the ammonia-oxidizing bacterium, *Nitrosomonas*

- etroptha* C91: implications for niche adaptation. *Environ Microbiol* 9:2993–3007. <https://doi.org/10.1111/j.1462-2920.2007.01409.x>.
51. Berg IA. 2011. Ecological aspects of the distribution of different autotrophic CO₂ fixation pathways. *Appl Environ Microbiol* 77:1925–1936. <https://doi.org/10.1128/AEM.02473-10>.
 52. Sedlacek CJ, McGowan B, Suwa Y, Sayavedra-Soto LA, Laanbroek HJ, Stein LY, Norton JM, Klotz MG, Bollmann A. 2019. A physiological and genomic comparison of *Nitrosomonas* cluster 6a and 7 ammonia-oxidizing bacteria. *Microb Ecol* 78:985–994. <https://doi.org/10.1007/s00248-019-01378-8>.
 53. Andrews TJ, Lorimer GH. 1978. Photorespiration—still unavoidable? *FEBS Lett* 90:1–9. [https://doi.org/10.1016/0014-5793\(78\)80286-5](https://doi.org/10.1016/0014-5793(78)80286-5).
 54. Badger MR, Bek EJ. 2008. Multiple RuBisCo forms in proteobacteria: their functional significance in relation to CO₂ acquisition by the CBB cycle. *J Exp Bot* 59:1525–1541. <https://doi.org/10.1093/jxb/erm297>.
 55. Goreau TJ, Kaplan WA, Wofsy SC, McElroy MB, Valois FW, Watson SW. 1980. Production of NO₂⁻ and N₂O by nitrifying bacteria at reduced concentrations of oxygen. *Appl Environ Microbiol* 40:526–532.
 56. Prieto-Alamo MJ, Jurado J, Gallardo-Madueno R, Monje-Casas F, Holmgren A, Pueyo C. 2000. Transcriptional regulation of glutaredoxin and thioredoxin pathways and related enzymes in response to oxidative stress. *J Biol Chem* 275:13398–13405. <https://doi.org/10.1074/jbc.275.18.13398>.
 57. Coulter ED, Kurtz DM, Jr. 2001. A role for rubredoxin in oxidative stress protection in *Desulfovibrio vulgaris*: catalytic electron transfer to rubrerythrin and two-iron superoxide reductase. *Arch Biochem Biophys* 394:76–86. <https://doi.org/10.1006/abbi.2001.2531>.
 58. Andrews SC, Robinson AK, Rodríguez-Quiriones F. 2003. Bacterial iron homeostasis. *FEMS Microbiol Rev* 27:215–237. [https://doi.org/10.1016/S0168-6445\(03\)00055-X](https://doi.org/10.1016/S0168-6445(03)00055-X).
 59. Rouhier N, Couturier J, Johnson MK, Jacquot JP. 2010. Glutaredoxins: roles in iron homeostasis. *Trends Biochem Sci* 35:43–52. <https://doi.org/10.1016/j.tibs.2009.08.005>.
 60. Wei X, Sayavedra-Soto LA, Arp DJ. 2004. The transcription of the *ccb* operon in *Nitrosomonas europaea*. *Microbiology* 150:1869–1879. <https://doi.org/10.1099/mic.0.26785-0>.
 61. Lorimer GH. 1981. The carboxylation and oxygenation of ribulose 1,5-bisphosphate: the primary events in photosynthesis and photorespiration. *Annu Rev Plant Physiol* 32:349–382. <https://doi.org/10.1146/annurev.pp.32.060181.00205.2>.
 62. McNevin D, von Caemmerer S, Farquhar G. 2006. Determining RuBisCO activation kinetics and other rate and equilibrium constants by simultaneous multiple non-linear regression of a kinetic model. *J Exp Bot* 57:3883–3900. <https://doi.org/10.1093/jxb/erl156>.
 63. Jiang D, Khunjar WO, Wett B, Murthy SN, Chandran K. 2015. Characterizing the metabolic trade-off in *Nitrosomonas europaea* in response to changes in inorganic carbon supply. *Environ Sci Technol* 49:2523–2531. <https://doi.org/10.1021/es5043222>.
 64. Terry KR, Hooper AB. 1970. Polyphosphate and orthophosphate content of *Nitrosomonas europaea* as a function of growth. *J Bacteriol* 103:199–206.
 65. Arp DJ, Sayavedra-Soto LA, Hommes NG. 2002. Molecular biology and biochemistry of ammonia oxidation by *Nitrosomonas europaea*. *Arch Microbiol* 178:250–255. <https://doi.org/10.1007/s00203-002-0452-0>.
 66. Sayavedra-Soto LA, Hommes NG, Russell SA, Arp DJ. 1996. Induction of ammonia monooxygenase and hydroxylamine oxidoreductase mRNAs by ammonium in *Nitrosomonas europaea*. *Mol Microbiol* 20:541–548. <https://doi.org/10.1046/j.1365-2958.1996.5391062.x>.
 67. Chandran K, Love NG. 2008. Physiological state, growth mode, and oxidative stress play a role in Cd(II)-mediated inhibition of *Nitrosomonas europaea* 19718. *Appl Environ Microbiol* 74:2447–2453. <https://doi.org/10.1128/AEM.01940-07>.
 68. Whittaker M, Bergmann D, Arciero D, Hooper AB. 2000. Electron transfer during the oxidation of ammonia by the chemolithotrophic bacterium *Nitrosomonas europaea*. *Biochim Biophys Acta* 1459:346–355. [https://doi.org/10.1016/S0005-2728\(00\)00171-7](https://doi.org/10.1016/S0005-2728(00)00171-7).
 69. Zorz JK, Kozłowski JA, Stein LY, Strous M, Kleiner M. 2018. Comparative proteomics of three species of ammonia-oxidizing bacteria. *Front Microbiol* 9:938. <https://doi.org/10.3389/fmicb.2018.00938>.
 70. Bollmann A, Sedlacek CJ, Norton J, Laanbroek HJ, Suwa Y, Stein LY, Klotz MG, Arp D, Sayavedra-Soto L, Lu M, Bruce D, Detter C, Tapia R, Han J, Woyke T, Lucas SM, Pitlucck S, Pennacchio L, Nolan M, Land ML, Hunt-emann M, Deshpande S, Han C, Chen A, Kyrpides N, Mavromatis K, Markowitz V, Szeto E, Ivanova N, Mikhailova N, Pagani I, Pati A, Peters L, Ovchinnikova G, Goodwin LA. 2013. Complete genome sequence of *Nitrosomonas* sp. Is79, an ammonia oxidizing bacterium adapted to low ammonium concentrations. *Stand Genomic Sci* 7:469–482. <https://doi.org/10.4056/signs.3517166>.
 71. Elmore BO, Bergmann DJ, Klotz MG, Hooper AB. 2007. Cytochromes P460 and c'-beta; a new family of high-spin cytochromes c. *FEBS Lett* 581:911–916. <https://doi.org/10.1016/j.febslet.2007.01.068>.
 72. Zahn JA, Arciero DM, Hooper AB, Dispirito AA. 1996. Cytochrome c' of *Methylococcus capsulatus* Bath. *Eur J Biochem* 240:684–691. <https://doi.org/10.1111/j.1432-1033.1996.0684h.x>.
 73. Liu S, Han P, Hink L, Prosser JI, Wagner M, Brüggemann N. 2017. Abiotic conversion of extracellular NH₂OH contributes to N₂O emission during ammonia oxidation. *Environ Sci Technol* 51:13122–13132. <https://doi.org/10.1021/acs.est.7b02360>.
 74. Zumft WG. 1997. Cell biology and molecular basis of denitrification. *Microbiol Mol Biol Rev* 61:533–616.
 75. Bueno E, Mesa S, Bedmar EJ, Richardson DJ, Delgado MJ. 2012. Bacterial adaptation of respiration from oxic to microoxic and anoxic conditions: redox control. *Antioxid Redox Signal* 16:819–852. <https://doi.org/10.1089/ars.2011.4051>.
 76. Sousa FL, Alves RJ, Pereira-Leal JB, Teixeira M, Pereira MM. 2011. A bioinformatics classifier and database for heme-copper oxygen reductases. *PLoS One* 6:e19117. <https://doi.org/10.1371/journal.pone.0019117>.
 77. Hino T, Matsumoto Y, Nagano S, Sugimoto H, Fukumori Y, Murata T, Iwata S, Shiro Y. 2010. Structural basis of biological N₂O generation by bacterial nitric oxide reductase. *Science* 330:1666–1670. <https://doi.org/10.1126/science.1195591>.
 78. Sousa FL, Alves RJ, Ribeiro MA, Pereira-Leal JB, Teixeira M, Pereira MM. 2012. The superfamily of heme-copper oxygen reductases: types and evolutionary considerations. *Biochim Biophys Acta* 1817:629–637. <https://doi.org/10.1016/j.bbabi.2011.09.020>.
 79. Giuffrè A, Stubauer G, Sarti P, Brunori M, Zumft WG, Buse G, Soulimane T. 1999. The heme-copper oxidases of *Thermus thermophilus* catalyze the reduction of nitric oxide: evolutionary implications. *Proc Natl Acad Sci U S A* 96:14718–14723. <https://doi.org/10.1073/pnas.96.26.14718>.
 80. Forte E, Urbani A, Saraste M, Sarti P, Brunori M, Giuffrè A. 2001. The cytochrome *ccb3* from *Pseudomonas stutzeri* displays nitric oxide reductase activity. *Eur J Biochem* 268:6486–6491. <https://doi.org/10.1046/j.0014-2956.2001.02597.x>.
 81. Pereira MM, Teixeira M. 2004. Proton pathways, ligand binding and dynamics of the catalytic site in haem-copper oxygen reductases: a comparison between the three families. *Biochim Biophys Acta* 1655:340–346. <https://doi.org/10.1016/j.bbabi.2003.06.003>.
 82. Han H, Hemp J, Pace LA, Ouyang H, Ganesan K, Roh JH, Daldal F, Blanke SR, Gennis RB. 2011. Adaptation of aerobic respiration to low O₂ environments. *Proc Natl Acad Sci U S A* 108:14109–14114. <https://doi.org/10.1073/pnas.1018958108>.
 83. Matsuda Y, Inamori KI, Osaki T, Eguchi A, Watanabe A, Kawabata SI, Iba K, Arata H. 2002. Nitric oxide-reductase homologue that contains a copper atom and has cytochrome c-oxidase activity from an aerobic phototrophic bacterium *Roseobacter denitrificans*. *J Biochem* 131:791–800. <https://doi.org/10.1093/oxfordjournals.jbchem.a003167>.
 84. Zumft WG. 2005. Nitric oxide reductases of prokaryotes with emphasis on the respiratory, heme-copper oxidase type. *J Inorg Biochem* 99:194–215. <https://doi.org/10.1016/j.jinorgbio.2004.09.024>.
 85. Füssel J, Lückler S, Yilmaz P, Nowka B, van Kessel M, Bourceau P, Hach PF, Littmann S, Berg J, Spieck E, Daims H, Kuypers MMM, Lam P. 2017. Adaptability as the key to success for the ubiquitous marine nitrite oxidizer *Nitrocooccus*. *Sci Adv* 3:e1700807. <https://doi.org/10.1126/sciadv.1700807>.
 86. Hood-Nowotny R, Umama NHN, Inselbacher E, Oswald-Lachouani P, Wanek W. 2010. Alternative methods for measuring inorganic, organic, and total dissolved nitrogen in soil. *Soil Sci Soc Am J* 74:1018–1027. <https://doi.org/10.2136/sssaj2009.0389>.
 87. Li B, Ruotti V, Stewart RM, Thomson JA, Dewey CN. 2010. RNA-Seq gene expression estimation with read mapping uncertainty. *Bioinformatics* 26:493–500. <https://doi.org/10.1093/bioinformatics/btp692>.
 88. Götz F, Pjevac P, Markert S, McNichol J, Becher D, Schweder T, Mussmann M, Sievert SM. 2019. Transcriptomic and proteomic insight into the mechanism of cyclooctasulfur- versus thiosulfate-oxidation by the chemolithoautotroph *Sulfurimonas denitrificans*. *Environ Microbiol* 21:244–258. <https://doi.org/10.1111/1462-2920.14452>.